ELSEVIER

Applied Catalysis A: General 174 (1998) 221–229

APPLIED CATALYSIS A: GENERAL

Hydrotalcite-supported palladium catalysts
Part I: Preparation, characterization of hydrotalcites and palladium on uncalcined hydrotalcites for CO chemisorption and phenol hydrogenation

S. Narayanan*, K. Krishna

Catalysis Section, Indian Institution of Chemical Technology, Hyderabad 500 007, India

Received 12 January 1998; received in revised form 23 February 1998; accepted 23 May 1998

Abstract

Hydrotalcites (HTs) are prepared by low supersaturation and high supersaturation methods, containing CO_3^{2-}, Cl^-, SO_4^{2-} interlayer anions and with different Al(III)/Al(III)+Mg(II) (x=0.33 and 0.25) ratios. Palladium hydrotalcite catalysts are obtained by impregnation of $PdCl_2$ aqueous solution on HTs. Different precursors of palladium are used for loading the metal onto HT prepared at high supersaturation. HT and palladium HTs are well characterized by XRD, surface area, IR, SEM, DTA. CO chemisorption is used to estimate palladium dispersion and metal area. The activity is evaluated for phenol hydrogenation reaction. The selectivity to cyclohexanone is always $\geq$90% even though phenol conversion varies with metal area.

Keywords: Hydrotalcite; Palladium; Phenol hydrogenation; Cyclohexanone

1. Introduction

Supported palladium catalysts are widely used for hydrogenation of many organic compounds. Support plays an important role in dispersing the active metal and giving stability to them in addition to influencing the catalytic properties [1]. The nature of support and the method of preparation certainly affect the morphology and the particle size and distribution which, in turn, will affect the catalytic properties. Even though many inorganic oxide materials have been used for supporting various metals, the search for new supports is still on for understanding the metal–support interaction and dispersion of metals. Using these catalysts for selective synthesis of chemicals at optimum activity levels is, of course, the final objective.

Hydrotalcites (HTs), a new class of basic mixed hydroxides, is being tried as supports for dispersing noble metals [2–5]. HT-like compounds, a layered double hydroxide of M(II) and M(III) cations having not too different a radius, in which the net positive charge is compensated by anions (mostly CO_3^{2-}) have proved to be good precursors for preparing hydrogenation catalysts [6]. Very little information is available concerning the catalytic activity of layered double

*Corresponding author. Fax: +91-40-717-3757; e-mail: root@c-siict.ren.nic.in

0926-860X/98/$ – see front matter
PII: S0926-860X(98)00190-2

hydroxide (LDH) carbonate [7]. Although many base catalysed reactions have been carried out over calcined HTs [8–11], there is only a limited information available on the noble metal supported on HTs and their use as hydrogenation catalysts.

Basile et al., [12] have reported homogeneous distribution of noble metals inside the precursor structure which, on further calcination and reduction, gave rise to well-dispersed and stable metal particles. Platinum and palladium supported on stabilised MgO were shown to be good catalysts in aromatisation reactions. Platinum clusters supported on stabilised magnesia catalysed the aromatisation of *n*-hexane with nearly the same activity and selectivity to benzene in preference to Pt-zeolite L. An unusually high selectivity to aromatics is observed for Pd supported on Al-stabilised MgO [3–5].

Catalytic hydrogenation of phenol is an important industrial route of preparing cyclohexanone which is an intermediate for the production of nylon-6. Industrially, this reaction is carried out over Pd/Al_2O_3 catalysts modified with alkali or alkali-earth metals [13] and many of the reports are concerned with the kinetics [14–16]. In a preliminary report [2], we have mentioned the high phenol hydrogenation activity of Pd/UHT catalysts and compared it with Pd/Al_2O_3 and Pd/MgO. The aim of the present work is to obtain further information on palladium supported on HTs and on the preparation methods of the supports as well as the catalysts. We describe here the use of uncalcined HT materials as supports for palladium. Mg–Al–HT is prepared by different methods by varying Al(III)/Al(III)+Mg(II) ratios and the interlayer anions. The supports and palladium-supported catalysts are well characterised. The structural features of HT on metal dispersion, CO adsorption and phenol hydrogenation are discussed in detail.

2. Experimental

2.1. Hydrotalcite materials

2.1.1. a) At high supersaturation with interlayer CO_3^{2-} (HT1 to HT4)

Hydrotalcite was prepared according to the method given in reference [17]. Solution A was prepared by dissolving 256 g of $Mg(NO_3)_2{\cdot}6H_2O$ and 185.7 g of $Al(NO_3)_3{\cdot}9H_2O$ in 700 cm^3 distilled water. Solution B was prepared by dissolving 280 g of 50% NaOH (140 g) and 100 g of Na_2CO_3 in 1000 cm^3 distilled water. HT1 was prepared by adding solution A to solution B in 3–4 h and crystallised at 333 K/18 h. Another HT sample was prepared by adding solution A to solution B in 8–9 h. It was divided into three parts and crystallisation was done at 333 K/18 h, 473 K/18 h and 473 K/45 h, respectively, and the samples were termed HT2, HT3 and HT4. The samples were filtered and washed several times with hot distilled water until the pH was neutral.

For the samples HT1 to HT4, x=Al(III)/Al(III)+Mg(II)=0.33.

2.1.2. b) At low supersaturation with interlayer CO_3^{2-} (HT5 and HT6)

Solution A was prepared by dissolving 64 g of $Mg(NO_3)_2{\cdot}6H_2O$ and 46.75 g of $Al(NO_3)_3{\cdot}9H_2O$ in 500 cm^3 distilled water. Solution B was prepared by dissolving 64 g of $Mg(NO_3)_2{\cdot}6H_2O$ and 31.2 g of $Al(NO_3)_3{\cdot}9H_2O$ in 500 cm^3 distilled water. Solution C was prepared by dissolving 40 g of NaOH and 21.2 g of Na_2CO_3 in 500 cm^3 distilled water. A and C were added simultaneously to the beaker containing 300 cm^3 of distilled water. The pH was maintained between 9 and 10 by adjusting the addition of A and C. Crystallisation was done at 333 K/18 h and the sample was termed HT5. Similarly, solution B is added to solution C by maintaining pH between 9–10 and the crystallisation was done at 333 K/18 h and the sample was termed HT6. For HT5, x=0.33 and for HT6, x=0.25. The materials were filtered and washed with hot distilled water until the pH was neutral.

2.1.3. c) At low supersaturation with interlayer HCO_3^- and SO_4^{2-}

HT7 and HT9 with interlayer HCO_3^-, CO_3^{2-} and SO_4^{2-}, respectively, were prepared by a method analogous to the HT6 with carbonate interlayer anion, except that $NaHCO_3$ and Na_2SO_4 were used instead of Na_2CO_3 in order to get x=0.25.

2.1.4. d) At low supersaturation with interlayer Cl^-, CO_3^{2-}

Synthesis of HT8 with interlayer Cl^-, CO_3^{2-} was carried out by previously described methods [18].

Table 1
Preparation conditions and surface area of hydrotalcites

Sample	$x = \frac{Al(III)}{Al(III)+Mg(II)}$	Supersaturation level	Crystallisation temp./time (K/h)	Interlayer anion	Surface area ($m^2\ g^{-1}$)
HT1	0.33	H [a]	333/18	CO_3^{2-}	90
HT2	0.33	H [a]	333/18	CO_3^{2-}	60
HT3	0.33	H [a]	473/18	CO_3^{2-}	32
HT4	0.33	H [a]	473/45	CO_3^{2-}	17
HT5	0.33	L [b]	333/18	CO_3^{2-}	66
HT6	0.25	L [b]	333/18	CO_3^{2-}	60
HT7	0.25	L [b]	333/18	HCO_3^-, CO_3^{2-}	78
HT8	0.25	L [b]	333/18	Cl^-, CO_3^{2-}	73
HT9	0.25	L [b]	333/18	SO_4^{2-}	2

[a] High supersaturation (pH $\geq$13).
[b] Low supersaturation (pH =10).

Table 1 gives the preparation conditions and surface area of the hydrotalcites prepared.

2.2. Pd on HT

Onto HT supports, prepared by various methods and with different interlayer anions, $PdCl_2$ acidified with HCl (to effect the complete dissolution of the salt) was impregnated so as to get the required weight percentages of metal. Different palladium precursors were used to load 1 wt% of Pd on HT2 support.

2.3. Characterisation

X-ray powder diffraction patterns were recorded with a Philips 1051 X-ray diffractometer with nickel filtered CuK_α radiation (λ=1.5405 A°). DTA of the samples were recorded using Leeds and Notrhrup (USA) instrument at a heating rate of 10 K min^{-1} in air. Infrared spectra were recorded with a Perkin–Elmer FT-IR instrument using KBr pellet technique. SEM pictures were taken using Hitachi S-800. Surface area was measured using nitrogen as adsorbate (30% N_2/70% He mixture) at 77 K with Micromeritics pulse chemisorb 2700 unit. Irreversible CO uptake was measured at room temperature on a reduced Pd/HT sample (573 K/3 h in H_2) in an all-glass high-vacuum volumetric system by double isotherm method, as described earlier [2]. A stoichiometry of Pd/CO=1 and a Pd surface density of 1.27×10^{19} atoms m^{-2} were assumed for calculating metal area and dispersion [14]. Average metal particle sizes, assuming spherical shapes for Pd particles, were calculated by using the equation $d=6V/S$, where S is the surface area of the metal and V the volume of palladium (7.9×10^{-29} m^3 $atom^{-1}$).

2.4. Phenol hydrogenation

Vapour-phase hydrogenation of phenol was studied over ca. 0.2 g of Pd/HT catalysts at 453 K in a vertical down-flow reactor. Before catalysis, the samples were reduced in hydrogen at 573 K for 3 h. The reaction mixture containing phenol and cyclohexane as diluent (1 : 4 wt/wt) was added from the top of the reactor at a controlled rate (WHSV=0.037 mol h^{-1} g^{-1} of phenol) with the help of a calibrated motorised syringe. H_2/phenol mole ratio was maintained at 4. The reaction products were analysed on a Chemito 3865 chromatograph with an Apiezon L treated with 2% KOH (2 m long) column. The experimental setup and conditions are given elsewhere [19].

3. Results and discussions

3.1. XRD

Typical XRD patterns of some HT samples are shown in Fig. 1. A well-crystallised HT structure is present in all the samples without any significant effect of supersaturation level [20]. Sharp and symmetrical peaks for (003), (006), (110) and (113) are observed for all the HT samples (except HT9). The

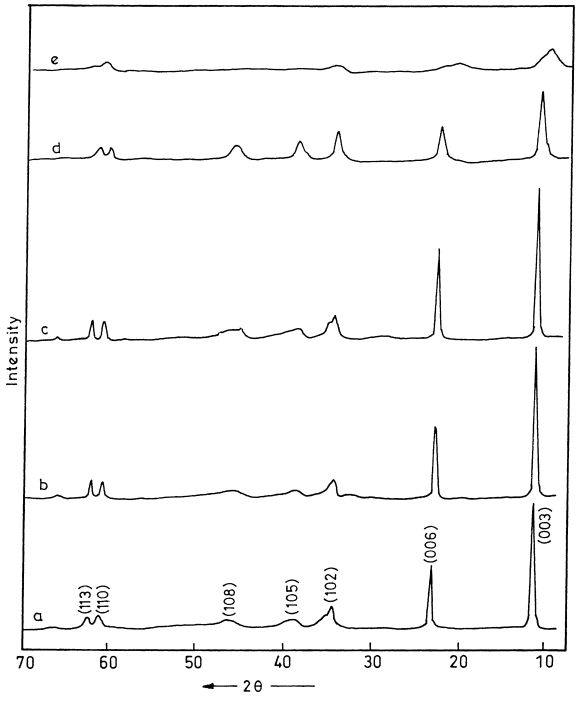

Fig. 1. XRD patterns of (a) HT2, (b) HT3, (c) HT4, (d) HT5 and (e) HT9.

peaks corresponding to (102), (105) and (108) are diffused and asymmetrical for the HT samples prepared at a high supersaturation (HT2, HT3 and HT4) and are relatively sharp and symmetrical for samples prepared at low supersaturation (HT5). HT3 and HT4, which were hydrothermally treated, showed more intense and sharp basal reflections relative to HT2 aged at 333 K and may be due to the larger crystallite size. The crystal size and perfection depend on the time and temperature of crystallisation. As for example, at 333 K/18 h, imperfect laminar particles are obtained, whereas at 473 K well-developed hexagonal crystals are produced [17]. The crystallinity of the materials enhances with treatment temperature and time due to the agglomeration of small particles leading to large crystallites. The intensity of the higher angular non-basal reflections are broad and asymmetric for HT2, HT3 and HT4, thus indicating a partially disordered structure. Even though the crystallite size is expected to be large for the HT5, prepared at pH=10, it showed the presence of relatively broad (003) and (006) basal reflections indicating disorder in the stacking of the layers. The well-developed, sharp non-basal reflections for HT5 indicate the presence of a fully disordered sub-cell arising from the indeterminate type of packing [6]. The well-developed (*0kl*) reflections are assigned for two modifications with different stacking orders present, having doubled and tripled *c*-axis, respectively. A large part of the HT sample is expected to have the latter [21]. Minerals with a similar structure of HT are known and also can be prepared with x in the 0.25–0.33 range. The coalingite structure consists of two or three brucite-type layers for every interlayer [22]. For the HT prepared at pH=10 and x=0.33, Corma et al., [23] have found different phases corresponding to different stacking and interlayer hydroxyl anion. However, we did not observe any secondary phases in HT5. All the other supports with different interlayer anions showed good HT structure. HT9 with interlayer SO_4^{2-} anion showed XRD pattern of quasi-amorphous compound. The crystallographic parameters of HT, calculated for hexagonal cell are in good agreement with the previous reports [22–24]. For HT1, a=3.044 and c=7.582, and for HT6, a=3.078 and c=7.816, indicating the isomorphous substitution of Mg^{2+} in the brucite-like sheet of HT by Al^{3+}.

3.2. DTA

DTA of HT samples (Fig. 2) show two endothermic peaks corresponding to weight loss. The peak around 473 K corresponds to both, the liberation of interparticle (physisorbed) and interlayer water which cannot be distinguished. The peak ca. 733 K is due to dehydroxylation of brucite layer and to the loss of carbon dioxide from the interlayer anion. The loss of interlayer water starts at 498 K for the hydrotalcites prepared by the high-supersaturation method (HT2). This is indicative of strongly bound interlayer water molecules in hydrotalcite prepared at high supersaturation. In HT9, the loss of SO_4^{2-} and dehydroxylation of brucite layer occur at slightly higher temperatures. The relative intensity of the endothermic peak, corresponding to the loss of interlayer water, is low in HT6 compared to HT2 or HT5, indicating the difference in interlayer water molecules. This is possibly due to the difference in Mg/Al ratios of the HTs. DTA analysis otherwise confirms the absence of any impurity phases in hydrotalcite sample.

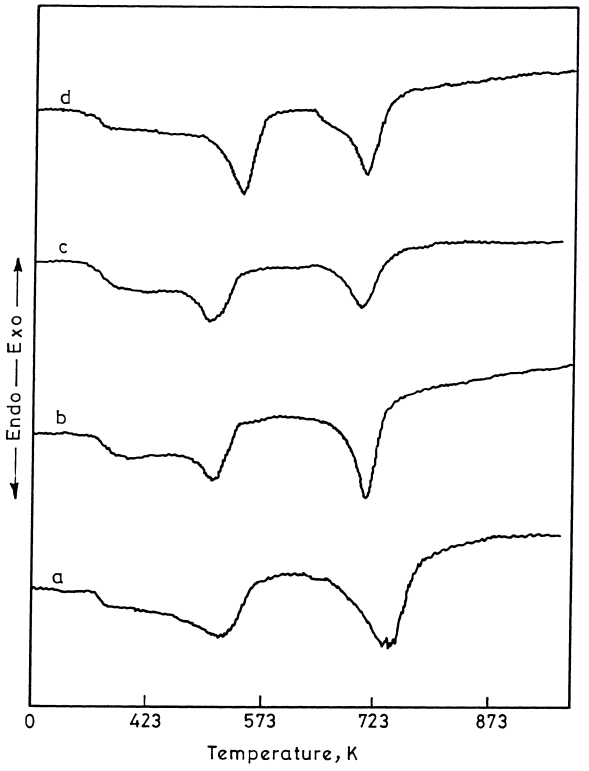

Fig. 2. DTA curves of (a) HT9, (b) HT6, (c) HT5 and (d) HT2.

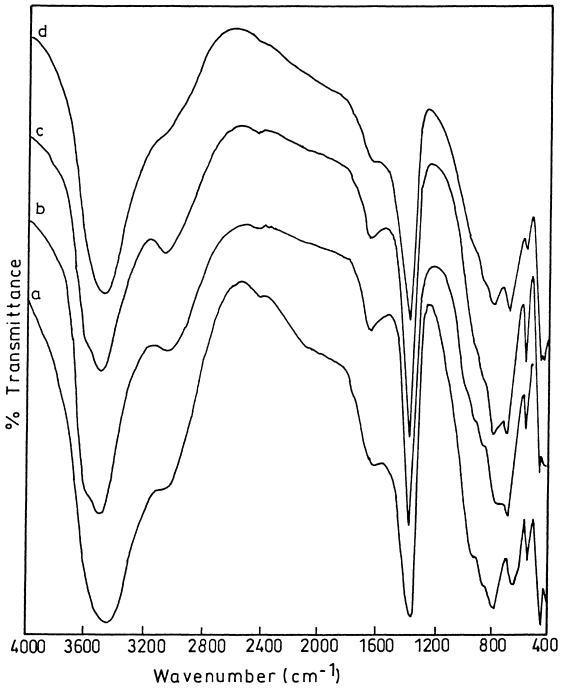

Fig. 3. IR spectra of (a) HT2, (b) HT3, (c) HT4 and (d) HT5.

3.3. IR spectra

FT-IR spectra of HTs (Fig. 3) reveal a strong absorption band at 3357 cm^{-1} for ν_{OH} stretching, indicating that hydroxyl groups of a brucite-like layer are hydrogen bonded. A weak band at 3080 cm^{-1} is due to the water-molecule hydrogen bonded to the carbonate ion present in the interlayer. Water-bending vibration occurs at 1600 cm^{-1}. The three absorption bands observed at 1365, 868, and 644 cm^{-1} indicate that the carbonate anion is in an asymmetric environment characterised by D3h planar symmetry. Some of the peaks in the 400–1000 cm^{-1} region are assigned due to lattice vibrations such as M(II)–M(III)–O, M–O– bending and stretching vibrations [25].

Analysis of the spectra in the 3400–3800 cm^{-1} region shows that, for the hydrotalcite prepared at high supersaturation and crystallised at 333 K, the ν_{OH} is broad and asymmetrical (HT2). For the sample prepared at low supersaturation (HT5) and on hydrothermally treated HT3, HT4 and HT5, the half-width becomes narrow and the intensity of the band decreases. The decrease in half-width indicates more orderliness of the cation distribution inside the brucite-like sheet [6]. A band is observed at 3600 cm^{-1} for the hydrothermally treated samples (HT3, HT4). This band could be due to the severe conditions of the hydrothermal treatment which may result in the hydroxyl groups associated with the oxides of magnesium and aluminium [26–28]. For the hydrothermally treated HTs, and the HTs prepared at low supersaturation, the band at 1365 cm^{-1} is sharp indicating the orderliness of the anion in the interlayer [25]. In HT2 and HT5, the differences can be observed in peak intensities of water-bending vibration (1600 cm^{-1}) and the shoulder (3080 cm^{-1}) corresponding to water-molecule hydrogen bonded to carbonate anion. The water-bending peak shifts slightly towards higher wave numbers in HT5. This difference in intensities and shifts could be due to the different amounts of interlayer water and the strength with which the water molecules are hydrogen bonded to the carbonate anion in the interlayer. This is also substantiated by DTA which showed a high-tempera-

ture shift towards interlayer water loss. A shift in the peak corresponding to ν_{OH} towards higher wave numbers is observed, as previously reported, for the HTs with different Mg/Al ratios [6].

3.4. SEM

The SEM pictures of HT1 (prepared at high supersaturation) and hydrothermally treated samples (HT3 and HT4) revealed small, thin platelets forming irregularly shaped aggregates. The sample prepared at low supersaturation (HT5) showed typically big platelets which are bundled together to form large clusters. HTs prepared at low supersaturation generally form large particles.

3.5. BET surface area

Hydrotalcites HT1 to HT4 were prepared at high supersaturation conditions. HT1 and HT2 differ in the surface area and it could be due to the difference in precipitation times employed in the preparation of these hydrotalcites: 3–4 h for HT1 and 8–9 h for HT2. The surface area of HT2 decreases from 60 to 32 $m^2\ g^{-1}$ (HT3) and to 17 $m^2\ g^{-1}$ (HT4) on hydrothermal treatment for different times (Table 1). The decrease in surface area is attributed to the increased particle size of the hydrotalcite. All the other hydrotalcites have showed a surface area of ca. 70 $m^2\ g^{-1}$, except HT9 which showed a surface area of 2 $m^2\ g^{-1}$.

4. Adsorption and catalytic activity

4.1. Influence of metal loading

CO chemisorption data on the Pd/HT1 samples prepared by $PdCl_2$ impregnation are given in Table 2. CO uptake increases with increase in metal content from 0.25 to 2 wt% over HT1 while the palladium dispersion decreases from 83 to 43% and the average crystallite size increases from 1.4 to 2.6 nm. CO uptake is more on Pd supported on HT1 than on alumina- or magnesia-supported catalysts. The variation in palladium dispersion over HT1, MgO and Al_2O_3 could be explained as due to the differences in the interaction of the anions of the precursor palladium salt with the support. Acidification of $PdCl_2$ leads to the $PdCl_4^{2-}$ and on impregnation over HT, the anion will be deposited on the external edge surface by replacing the carbonate anion leading to fine dispersion of the palladium precursor. On reduction, this gives highly dispersed small palladium particles compared to Pd/MgO and Pd/Al_2O_3. As the loading increases, the deposition will be more on the external surface of HT resulting in a shorter distance between metallic species and promoting sintering leading to the decreased dispersion. The deposition of palladium precursor in the internal surface can be ruled out as there is no shift in basal $d_{(003)}$ reflection in Pd/HT catalysts.

Table 2
Effect of metal loading over HT1 on CO adsorption properties

Pd (wt%)	CO uptake (cm^3 (g cat)$^{-1}$)	Pd dispersion (%)	Pd crystallite size (nm)
0.25	0.44	83	1.4
0.50	0.80	76	1.5
1.0	1.45	69	1.6
2.0	1.80	43	2.6
2wt%Pd/Al_2O_3 [a]	0.38	9	12.4
2.0wt%Pd/MgO [b]	0.56	13	8.6

[a] [2].
[b] Precursor $PdCl_2$.

In Fig. 4, the influence of metal content on metal area, conversion and selectivity for phenol hydrogenation is given. The increase in metal content from 0.25 to 2 wt% on HT1 increases MSA and the crystallite size (from 1.4 to 2.6 nm). The conversion of phenol increases from 25 to nearly 100% due to the increased metal availability. The selectivity for cyclohexanone, however, decreases slightly and it remains nearly 90% at all conversion levels. The turnover number for phenol hydrogenation does not change very much, suggesting that the activity of an exposed palladium metal atom per second is constant, irrespective of the metal content. There is no appreciable effect of crystallite size on the turnover number, indicating the structure-insensitive nature of the reaction. Palladium supported on hydrotalcite was found to be more active (conversion 100%) than 2 wt% Pd/Al_2O_3 and 2 wt% Pd/MgO which showed only 10 and 20% conversion, respectively. There was no deactivation with time-on-stream (4 h) over Pd/HT catalysts, whereas Pd supported on Al_2O_3 and MgO showed deactivation [2].

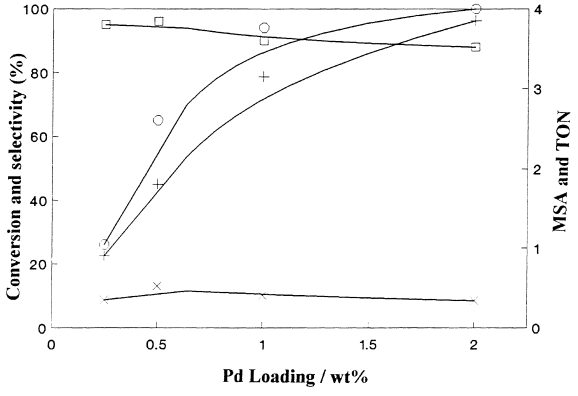

Fig. 4. Effect of palladium loading on (○) % conversion of phenol, (□) % selectivity of cyclohexanone, (+) metal surface area (m^2 (g cat)$^{-1}$) and (×) TON (s^{-1}).

4.2. Effect of precipitation conditions

Pd/HT1 and Pd/HT2 catalysts showed (Table 3) nearly equal CO uptakes (1.45–1.35 $cm^3\ g^{-1}$) although the surface areas of these HTs vary by 30 m^2g^{-1}. The palladium dispersion and crystallite size are ca. 69–64% and 1.6–1.7 nm, respectively. Similarly, palladium on HT3 and HT4 showed a variation in Pd dispersion of ca. 51–46% and in crystallite size of 2.2–2.4 nm. In spite of the fact that surface area is one of the factors that can affect the dispersion of the metal, the change in Pd dispersion is not commensurate with surface area change. Phenol hydrogenation follows the same trend as that of CO uptake. Pd/HT catalysts showed better conversion than Pd/Al_2O_3 or Pd/MgO [2]. The selectivity to cyclohexanone is 90% on all the catalysts, irrespective of the conversion levels.

4.3. Influence of preparation method and Mg/Al ratio

HT2 and HT5 have the same value of x=0.33, whereas for HT6, x=0.25 (Table 1). The surface area of the supports is in the range 60–66 m^2g^{-1}. The two different preparation methods of the hydrotalcite resulted in significantly different dispersions and activities of palladium (Table 3). Pd on HT2 resulted mainly in a dispersion of 64% and when palladium was supported on HT5 and HT6, it gave a dispersion of 29 and 33%, respectively. The phenol conversion is in reasonable agreement with the CO uptake. The difference in dispersion could be related to the hydrotalcite morphology and to the disordered nature of HTs. The XRD and SEM studies show that the morphologies of HT2, HT5 and HT6 prepared by different routes are different. It is known that, under the low supersaturation conditions, the crystallite growth is faster than the growth of nucleus [6]. The relative amounts of palladium deposited by replacing the carbonate anion will be more in the case of HT2 with small particle size and exposes a greater number of carbonate sites at the edges. HT5, with large particle size, exposes lesser number of carbonate sites and, because of slow diffusion, most of the precursor will be deposited on the external surface and, on reduction, results in low dispersion. Pd/HT6 showed slightly

Table 3
CO chemisorption and phenol conversion over 1wt% Pd/HTs

Support	CO uptake ($cm^3\ g^{-1}$)	Pd metal surface area (m^2 (g cat)$^{-1}$)	Pd dispersion (%)	Pd crystallite size (nm)	Phenol conversion (%)
HT1	1.45	3.07	69	1.6	94
HT2	1.35	2.86	64	1.7	90
HT3	1.07	2.27	51	2.2	76
HT4	0.97	2.05	46	2.4	70
HT5	0.60	1.27	29	3.8	50
HT6	0.69	1.46	33	3.4	60
HT7	0.66	1.40	31	3.6	50
HT8	0.41	0.86	20	5.6	26
HT9	0.20	0.42	10	11.2	5
MgO	0.20	0.42	10	11.2	18
Al_2O_3	0.26	0.55	12	9.3	10

better dispersion and activity than Pd/HT5. The small differences in dispersion could be due to irregular scattering of palladium on to the surface and also to the differences in morphology of these materials.

4.4. Influence of interlayer anions

The adsorption and catalytic activity data over the Pd/HT catalysts with x=0.25 and having different interlayer anions is also given in Table 3. HT7 was prepared by precipitating with base solution containing bicarbonate anion and both carbonate and bicarbonate anions may be present in the precipitates [20]. The dispersion and crystallite size of palladium, supported on HT6 and HT7, are almost the same. Though one would expect higher dispersion of Pd by easier and fast exchange of chloride ions compared to that of carbonate by $PdCl_4^{2-}$, the catalyst, Pd/HT8, with interlayer Cl^-, CO_3^{2-} shows low palladium dispersion. The reason for this may be that the external edge surface preferably has more carbonate anions than chloride anions leading to less dispersion. Pd/HT9 with SO_4^{2-} showed low Pd dispersion. Pd/HT6, Pd/HT7 and Pd/HT8 showed 60, 50 and 26% conversion, respectively. Pd/HT9 showed a conversion of only 5%. Palladium is highly sensitive to sulphur compounds [29]. The low conversion could be due to the low surface area of HT9 leading to low palladium dispersion and to a possible sulphur poisoning of palladium, resulting from SO_4^{2-} during reduction.

4.5. Effect of palladium precursor

Table 4 shows the effect of palladium precursor on CO uptake and the activity of 1 wt% Pd/HT2 prepared with different palladium precursors. The conversions and activities given in Table 4 were calculated based on the first 30 min product analysis. While these catalysts maintained activity for 4 h, Pd/Al_2O_3 showed deactivation with time [30]. It is clear that the catalysts prepared from anionic precursors show large CO uptake and high dispersion. The amine and acetate precursors which are generally used to get high dispersions over oxides [14] are poorly dispersed over HT2. This supports the fact that the interlayer carbonate anion is playing a major role in dispersing the palladium precursor. The hydrogenation activity changes over a wide range. The catalyst prepared with chloride precursor is more active (90%) than the one prepared by acetate (conversion 30%) or amine precursor (conversion 41%).

Now, 1 wt% Pd/Al_2O_3 catalyst prepared by using K_2PdCl_4 showed low CO uptake (0.2 cm^3g^{-1}) and the activity was 1.3×10^{-2} mol g^{-1} h^{-1}. Pd/HT2 catalyst prepared with K_2PdCl_4 as precursor showed a marked increase in activity (7.7×10^{-2} mol g^{-1} h^{-1}) compared to the one prepared by $PdCl_2$ precursor (3.5×10^{-2} mol $g^{-1}h^{-1}$). The catalytic performance of the alkali-doped palladium catalysts has been attributed to a modification of surface acid–base properties of the support [15]. The electronic effect, induced by alkali over Pd has also been emphasized by several authors [31]. The alkali promoter donates an electron to the metal, increasing the charge density over the palladium particle leading to different activities. In view of the small particle size of palladium on HT2 (catalyst D, 1.6 nm) the influence of electronic effect on the activity and selectivity of these catalysts to phenol hydrogenation cannot be precluded.

Table 4
Effect of Pd precursor on CO adsorption and catalytic activity of 1 wt% Pd catalysts

Sample	Precursor	Support	CO uptake cm^3g^{-1}	Pd Dispersion %	Pd Crystalite size, nm	Conversion %	Activity $molg^{-1}h^{-1}\times10^{-2}$
A	$PdCl_2$	HT2	1.35	64	1.7	90	3.5
B	$Pd(NH_3)_4Cl_2$	HT2	0.29	14	7.4	41	1.5
C	$Pd(CH_3COO)_2$	HT2	0.57	27	4.1	30	1.1
D [a]	K_2PdCl_4	HT2	1.40	67	1.6	78	7.7
E	$PdCl_2$	Al_2O_3	0.26	12	9.3	27	1.1
F	K_2PdCl_4	Al_2O_3	0.22	10	11.2	34	1.3

Weight of the catalyst for the reaction: 200 mg
[a] Weight of the catalyst for the reaction: 75 mg.

5. Conclusions

Uncalcined hydrotalcite was found to be good material for supporting palladium. The preparation method of hydrotalcite and the interlayer anions influence the dispersion and metal area of palladium in supported catalysts. HT1 prepared by the high-supersaturation method and with interlayer CO_3^{2-} anion was found to be better among all the catalysts, in terms of metal dispersion and phenol hydrogenation activity. The anionic palladium precursors impregnated over these hydrotalcite supports help dispersion as well as activity towards phenol hydrogenation. The selectivity to cyclohexanone was always >90% over these catalysts, even when phenol conversion varied with available Pd area. Pd/HT was found to be a better catalyst than Pd/Al_3O_3 and Pd/MgO for phenol hydrogenation.

Acknowledgements

K. Krishna thanks CSIR, New Delhi, for the award of a Senior Research Fellowship.

References

[1] F. Solymosi, Catal. Rev. 1 (1968) 252.
[2] S. Narayanan, K. Krishna, Appl. Catal. A. 147 (1996) L253.
[3] R.J. Davis, E.G. Derouane, Nature 349 (1991) 313.
[4] R.J. Davis, E.G. Derouane, J. Catal. 132 (1991) 269.
[5] I.I. Ivanova, A. Paran-Claerbout, M. Seirert, N. Blomend, E.G. Derouane, J. Catal. 158 (1991) 521.
[6] F. Cavani, F. Trifiro, A. Vaccari, Catal. Today 11 (1991).
[7] V.R.L. Constantino, T.J. Pinnavaia, Catal. Lett. 23 (1994) 361.
[8] A. Corma, V. Fornes, R.M. Martin-Aranda, F. Rey, J. Catal. 134 (1992) 58.
[9] W.T. Reichle, J. Catal. 94 (1985) 547.
[10] E. Suzukiand, Y. Ono, Bull. Chem. Soc. Jpn. 61 (1988) 1008.
[11] M.J. Climent, A. Corma, S. Iborra, J. Primo, J. Catal. 151 (1995) 60.
[12] F. Basile, L. Basini, G. Fornasari, M. Gazzano, F. Trifiro, A. Vaccari, Chem. Commun. (1996) 2435.
[13] I. Dodgson, K. Grifin, G. Barberis, F. Pignataro, G. Tausizik, Chem. Ind. (London), 830 (1981).
[14] S. Galvagno, A. Danata, G. Neri, R. Pietropalo, J. Chem. Tech. Bio. Technol. 51 (1991) 145.
[15] G. Neri, A.M. Visco, A. Donato, C. Milone, M. Malentacchi, G. Gabitosa, Appl. Catal. A. 110 (1994) 49.
[16] J.R. Gonzalez-Velasco, J.I. Gatierrez-Ortiz, J.A. Gonzalez-Marcos, A. Romero, React. Kinet. Catal. Lett. 32 (1986) 505.
[17] W.T. Reichle, S.Y. Kang, D.S. Everhardt, J. Catal. 101 (1986) 352.
[18] D. Tichit, M.H. Lhouty, A. Guida, B.H. Chiche, F. Figueras, A. Auroux, D. Bartalini, E. Garrone, J. Catal. 151 (1995) 50.
[19] S. Narayanan, G. Srikanth, React. Kinet. Catal. Lett. 51 (1993) 449.
[20] O. Clause, M. Gazzano, F. Trifiro, A. Vaccari, L. Zatroski, Appl. Catal. 73 (1991) 217.
[21] E.C. Kruissink, L.L. Van Reijen, J.R.H. Ross, J. Chem. Soc. Faraday Trans. 1(77) (1981) 649.
[22] H. Schaper, J.J. Berg-Slot, W.H.J. Stork, Appl. Catal. 54 (1989) 79.
[23] A. Corma, V. Fornes, F. Rey, J. Catal. 148 (1994) 205.
[24] G.H. Brindley, S. Kikkava, Am. Mineral. 64 (1979) 836.
[25] S. Kannan, S. Velu, V. Ramkumar, C.S. Swamy, J. Mater. Sci. 30 (1995) 1462.
[26] F. Rey, V. Fornes, J.M. Rojo, J. Chem. Soc. Faraday Trans. 88 (1992) 2233.
[27] M. Che, C. Naccache, B. Imelik, J. Catal. 24 (1972) 328.
[28] H. Knozinger, P. Ratnasamy, Catal. Rev., Sci. Eng. 17 (1978) 31.
[29] J.P. Boitiaux, J. Coryns, F. Verna, Stud. Surf. Sci. Catal. 34 (1987) 105.
[30] S. Narayanan, K. Krishna, Chem. Commun. (1997) 1991.
[31] L.F. Liotta, G.A. Marten, G. Deganello, J. Catal. 164 (1996) 322, and the references cited therein.